2001-01-4067

On the Errors Induced by the Hookean Modeling of Nominal Stresses in the εN Method

Marco Antonio Meggiolaro
Jaime Tupiassú Pinho de Castro
Mechanical Engineering Department
Pontifical Catholic University of Rio de Janeiro (PUC-Rio), Brazil
e-mails: meggi@mec.puc-rio.br, jtcastro@mec.puc-rio.br

ABSTRACT

The traditional εN procedures are inconsistent when modeling nominal stresses by Hooke's law and the stresses and strains at the critical notch root by Ramberg-Osgood's equation, since the material is the same at both regions. When the nominal stresses are not substantially smaller than the yielding strength S_Y, the predicted hysteresis loops at the notch root can be significantly ***non***-conservative. In fact, when the nominal stresses are in the order of S_Y, the Hookean model can predict stresses and strains at the notch root that are ***smaller*** than the nominal ones, a clear nonsense. To avoid this problem, it is mandatory to use Ramberg-Osgood to model both the nominal and the critical stresses and strains. However, this approach is not trivial to implement, especially when complex loads are involved. In this work, the methodology required to warrant correct numerical predictions of the critical loops under high nominal loads are discussed.

Keywords: Fatigue Design, Strain-Life Method, Neuber Rule, Complex Loading.

INTRODUCTION

Fatigue is the type of mechanical failure characterized by the generation and/or gradual propagation of a crack, caused primarily by the repeated application of variable loads. These phenomena are progressive, cumulative and localized.

The crack generation usually starts from a notch, and depends primarily on the range of the *local* stress ($\Delta\sigma$) or strain ($\Delta\varepsilon$) acting on the critical or most loaded point of the structure. For design purposes, $\Delta\sigma$ and $\Delta\varepsilon$ should be calculated on a volume large in comparison to the microstructural parameter which characterizes the material anisotropy (e.g., the grain size in metals). When the cyclic loads are large (causing macroscopic cyclic yielding), ductility is the main material fatigue strength controlling parameter.

When macroscopic cyclic yielding is present, the traditional method to design against fatigue crack initiation is the εN. This method is *local*, in the sense that its load history is completely described by the stress or strain acting at the critical point. In this manner, a strain gage and an appropriate stress concentration factor ($\mathbf{K_t}$) can provide all the loading information required to apply the εN design method. The fundamentals of the εN method to calculate fatigue damage caused by complex loading and its numerical implementation are discussed below.

CLASSICAL εN METHOD

The εN method correlates the number of cycles **N** to initiate a fatigue crack in any structure with the life (in cycles) of small specimens that should (i) have the same fatigue strength (hence, the same material and details) and (ii) be submitted to the same *strain* history that loads the structure critical point (generally a notch root) in service. Therefore, the εN and the SN methods are based in similar philosophies. As in the SN method, the εN method does not recognize the presence of cracks. However, the εN recognizes macroscopic elastic-plastic events at the notch roots and uses the local strain range (a more robust parameter to describe plastic effects) instead of the stress range to quantify them. The εN design routine is:

- to evaluate the critical point fatigue strength,
- to calculate the critical point strain history, considering strain concentration effects, and
- to quantify the damage accumulated by each load event.

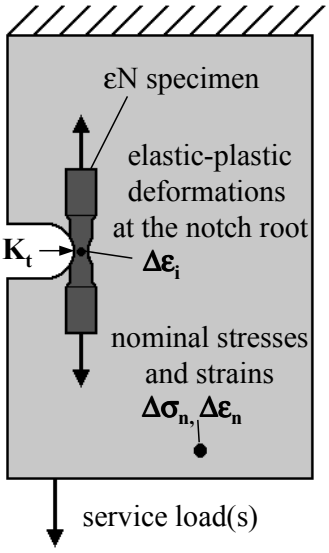

Figure 1. The philosophy of the εN method.

Macroscopic plastic strain ranges cyclically move dislocations and can quickly induce fatigue cracks. Hence, the low-cycle fatigue strength is much less influenced by the critical point details such as surface roughness and strain gradients than the high-cycle, and it is controlled primarily by the material ductility. The εN method must be used to model low cycle problems, when the plastic strain range $\Delta\varepsilon_p$ at the critical point is of the same order or larger than the elastic range $\Delta\varepsilon_e$, but it can be applied to predict any initiation life. This model requires 4 pieces of information:

1. a $\Delta\sigma$-$\Delta\varepsilon$ relationship, to describe the elastic-plastic hysteresis loops at the critical point;
2. a strain concentration rule, to correlate the nominal stress range $\Delta\sigma_n$ with the strain range $\Delta\varepsilon$ it induces at the critical notch root;
3. a $\Delta\varepsilon$-**N** relationship, to correlate the strain range $\Delta\varepsilon$ with the fatigue crack initiation life **N**; and
4. a damage accumulation model.

The classical εN method works with real (logarithmic) stresses and strains, uses a Ramberg-Osgood description for the $\Delta\sigma\Delta\varepsilon$ loops, and considers the cyclic softening or hardening of the material, but not its transient behavior from the monotonic σε curve [1-10]. Hence, a single equation is used in the εN method to describe all hysteresis loops

$$\varepsilon_a = \frac{\Delta\varepsilon}{2} = \frac{\Delta\varepsilon_e}{2} + \frac{\Delta\varepsilon_p}{2} = \frac{\Delta\sigma}{2E} + \left(\frac{\Delta\sigma}{2H_c}\right)^{1/h_c} \qquad (1)$$

where **E** is the Young's modulus, H_c is the hardening coefficient and h_c is the hardening exponent of the cyclically stabilized $\Delta\sigma\Delta\varepsilon$ curve.

Typical values for the cyclic hardening exponent h_c are typically between 0.05 and 0.3, while the monotonic hardening exponent **h** is more disperse, varying between 0 and 0.5. The hardening coefficient H_c is the value of the (real) stress that corresponds to a (real) plastic deformation of 100% on the cyclic curve or on its prolongation.

The Ramberg-Osgood relationship is well justified to predict the cyclic response of many materials, however it is only one of many empirical relations that can be used with this intention. Its main limitation is not to recognize a purely elastic behavior for very small strains, and its main advantage is its mathematical simplicity.

To correlate the nominal stress $\Delta\sigma_n$ and strain $\Delta\varepsilon_n$ ranges with the stress $\Delta\sigma$ and strain $\Delta\varepsilon$ ranges they induce at a notch root, a simplified version of the Neuber rule is used, which assumes elastic nominal loads

$$K_t^2 = \frac{\Delta\sigma \cdot \Delta\varepsilon \cdot E}{\Delta\sigma_n^2} \qquad (2)$$

Given $\Delta\sigma_n$, the material properties **E**, H_c and h_c, and the elastic stress concentration factor K_t, the notch root stress and strain ranges $\Delta\sigma$ and $\Delta\varepsilon$ are then calculated by an appropriate numerical algorithm. The relationship between the critical point stress range $\Delta\varepsilon$ and its fatigue initiation life **N** is usually given by the classical Coffin-Manson rule

$$\frac{\Delta\varepsilon}{2} = \frac{\sigma_c}{E}(2N)^b + \varepsilon_c(2N)^c \qquad (3)$$

where σ_c, ε_c, **b**, and **c** are material constants, which are normally measured in fully alternated traction-compression fatigue tests. The effect of a mean stress σ_m at the critical point is usually calculated by one of the three following rules:

$$\frac{\Delta\varepsilon}{2} = \frac{\sigma_c - \sigma_m}{E}(2N)^b + \varepsilon_c(2N)^c \qquad (4)$$

$$\frac{\Delta\varepsilon}{2} = \frac{\sigma_c - \sigma_m}{E}(2N)^b + \varepsilon_c\left(\frac{\sigma_c - \sigma_m}{\sigma_c}\right)^{c/b}(2N)^c \qquad (5)$$

$$\frac{\Delta\varepsilon}{2} = \frac{\sigma_c^2}{E \cdot \sigma_{max}}(2N)^{2b} + \frac{\sigma_c \cdot \varepsilon_c}{\sigma_{max}}(2N)^{b+c} \qquad (6)$$

Depending on the reference, equation (4) is called the Morrow and equation (5) the modified Morrow, or vice versa. To avoid this confusion, equation (4) may be called the Morrow elastic and equation (5) the Morrow elastic-plastic equation, while equation (6) is known as the Smith-Topper-Watson rule.

There is vast experimental support to justify the use of these εN equations to predict fatigue crack initiation under simple loads. However, when using this method under

complex loading, it is common to neglect loading order effects and to simply calculate the damage caused by the i-th load event as if it was independent of all others. Hence, the classical idea is to rain-flow count the nominal loads $\Delta\sigma_{ni}$, to calculate the corresponding notch root strain range $\Delta\sigma_i$ by

$$(K_t \Delta\sigma_{n_i})^2 = \Delta\sigma_i \cdot \left(\Delta\sigma_i + 2E \cdot \left(\frac{\Delta\sigma_i}{2H_c} \right)^{1/h_c} \right) \quad (7)$$

and to obtain the respective strain range $\Delta\varepsilon_i$ and damage d_i using

$$\frac{\Delta\sigma_i}{E} + 2 \cdot \left(\frac{\Delta\sigma_i}{2H_c}\right)^{\frac{1}{h_c}} = \Delta\varepsilon_i = \frac{2\sigma_c}{E}(2N_i)^b + 2\varepsilon_c(2N_i)^c$$

$$\Rightarrow d_i = \frac{n_i}{2N_i} \quad (8)$$

Despite its many shortcomings, most fatigue designers use the linear damage accumulation (or the Palmgren-Miner's) rule, $d = \Sigma d_i$, and predict failure when $\Sigma d_i = \beta$, with $\beta = 1$ being the most used value.

All above equations cannot be inverted, hence the use of the εN method is computationally difficult, explaining (but not justifying) the indiscriminate use of these equations, since

> *The application of these equations to the rain-flow count of the nominal loads usually does **not** generate predictions of physically acceptable hysteresis loops!*

LIMITATIONS OF THE CLASSICAL εN METHODOLOGY

The εN is a modern design method, corroborated by traditional institutions such as the SAE [9], but it has certain relatively little known idiosyncrasies. Particularly when dealing with complex loads, it is *not* possible to predict physically acceptable strain ranges at the critical point without recognizing the load *order*. Since plasticity generates memory, sequence effects must be accounted for when accurately modeling elastic-plastic hysteresis loops. In reality, precise fatigue life predictions require an accurate description of the stress-strain *history* at the critical point. In practice, such predictions can only be made with the aid of an appropriate automation software, since the numerical effort to sequentially solve the εN equations is quite heavy. Moreover, as the loop predictions are difficult, the software must have powerful graphical tools, to allow for the visual checking of the calculated hysteresis loops.

In fact, to guarantee the quality of the predictions it is indispensable to first assure that the calculation model reproduces the hysteresis loops at the critical point, for only then calculating the damage caused by the loops. Even if the piece is virgin, if the residual stress and strain state is zero, and if the cyclical hardening or softening transient can be neglected, the increments of plastic strain are dependent on the load history and it is necessary to distinguish the first 1/2 cycle from the subsequent load events. Even in the idealized case, the first 1/2 cycle departs from the origin of the σε plane following the (cyclic) σε curve and not the loop equation

$$(K_t \sigma_{n_0})^2 = \sigma_0 \cdot \left(\sigma_0 + E \cdot \left(\frac{\sigma_0}{H_c} \right)^{1/h_c} \right) \quad (9)$$

$$\frac{\sigma_0}{E} + \left(\frac{\sigma_0}{H'}\right)^{\frac{1}{h'}} = \varepsilon_0 = \frac{2\sigma'_f}{E}(2N_0)^b + 2\varepsilon'_f(2N_0)^c$$

$$\Rightarrow d_0 = \frac{1}{2N_0} \quad (10)$$

But this indispensable care is still not enough. It is also necessary to guarantee that all the subsequent events do not surpass (i) the cyclic σε curve, nor (ii) the wrapper of the hysteresis loops. Hence, the automation software should verify if and when the predicted strains (by the equation of the hysteresis loop applied for each load event $\Delta\sigma_i\Delta\varepsilon_i$) cross the cyclic σε curve or a previously induced loop. At the crossing point, the software must change the equation of that i-th event, and it must follow the cyclic σε curve or the curve of the previously induced loop until the end of that i-th load event.

The computational details of this complicated calculation step are considered beyond the scope of this paper, but are discussed elsewhere [11-13]. However, it is worth emphasizing that these corrections are indispensable under penalty of generating predictions that are (i) physically inadmissible, and (ii) probably *non*-conservative. Only after applying all the required corrections it is possible to predict decent loops and, hence, the correct fatigue damage if the load is complex.

However, the issues discussed above are not the only problems in the classical εN methodology. When dealing with stress concentration, it is common practice to model the nominal stresses as purely elastic, while using an elastic-plastic model such as Ramberg-Osgood to represent the behavior at the critical point. The next section shows that this approach may lead to highly non-conservative life predictions, and presents methods to deal with this problem.

LIMITATIONS OF THE CLASSICAL NEUBER APPROACH

Neuber is the most used rule to correlate the nominal stress $\Delta\sigma_n$ and strain $\Delta\varepsilon_n$ ranges with the stress $\Delta\sigma$ and strain $\Delta\varepsilon$ ranges they induce at a notch root. The Neuber rule states that the product between the stress concentration factor K_σ (defined as $\Delta\sigma/\Delta\sigma_n$) and the strain concentration factor K_ε (defined as $\Delta\varepsilon/\Delta\varepsilon_n$) is constant and equal to the square of the geometric stress concentration factor K_t, thus

$$K_t^2 = \frac{\Delta\sigma \cdot \Delta\varepsilon}{\Delta\sigma_n \cdot \Delta\varepsilon_n} \tag{11}$$

Some authors prefer to use K_f, the fatigue concentration factor instead of K_t in this equation [14]. When the nominal loads are elastic, it is common practice to use Neuber rule in the form

$$K_t^2 = \frac{\Delta\sigma \cdot \Delta\varepsilon \cdot E}{\Delta\sigma_n^2} \tag{12}$$

Using Ramberg-Osgood to correlate the stresses and strains at the notch root, equation (12) becomes

$$K_t^2\,\Delta\sigma_n^2 = \Delta\sigma^2 + \frac{2E\Delta\sigma^{(h_c+1)/h_c}}{(2H_c)^{1/h_c}} \tag{13}$$

However, this practice is logically incongruent, since it treats the same material by two different models: Ramberg-Osgood at the notch root and Hooke at the nominal region. This procedure can generate significant numerical errors even when the nominal stresses are much lower than the material yielding strength.

Consider for instance a specimen made of SAE 1015 steel, with hardening properties $h_c = 0.22$ and $H_c = 945$MPa [9]. Let's calculate the stress at a notch root with $K_t = 3$, associated with a nominal stress amplitude $\Delta\sigma_n/2$ of 380MPa. From equation (13),

$$3^2 \cdot 760^2 = \Delta\sigma^2 + \frac{2 \cdot 207000 \cdot \Delta\sigma^{(0.22+1)/0.22}}{(2 \cdot 945)^{1/0.22}} \tag{14}$$

which results in $\Delta\sigma/2 \cong 375\text{MPa} < 380\text{MPa}$! This result is a clear non-sense, since the stresses at the notch root must always be greater than the nominal ones (in modulus).

There are two basic procedures to avoid the errors induced by equation (13). The first procedure is to abandon the Ramberg-Osgood modeling of the material hardening and use a more appropriate model that recognizes pure elastic strains. Ramberg-Osgood considers plastic strains even for very small applied stresses, which is not physically reasonable since pure elastic behavior is expected in these cases. To recognize pure elastic strains, a different stress-strain relationship must be considered, for instance

$$\varepsilon = \begin{cases} \sigma/E, & \sigma \le \sigma_Y \\ \dfrac{\sigma}{E} + \left[\dfrac{\sigma - \sigma_Y}{H_p}\right]^{1/h_p}, & \sigma > \sigma_Y \end{cases} \tag{15}$$

where H_p and h_p are hardening parameters, and σ_Y is the highest stress associated with no residual plastic strain ($\varepsilon_{pres} = 0$). Note that σ_Y is always smaller than the material yielding strength S_Y, since the latter is in general defined by a residual plastic strain ε_{pres} of 0.2%. If the considered nominal stresses are below σ_Y, and if equation (15) can be applied to represent the notch root hysteresis loops, then Neuber's equation can be written as

$$K_t^2\,\Delta\sigma_n^2 = \begin{cases} \Delta\sigma^2, & \Delta\sigma \le 2\sigma_Y \\ \Delta\sigma^2 + 2E\Delta\sigma\left[\dfrac{\Delta\sigma - 2\sigma_Y}{2H_p}\right]^{1/h_p}, & \Delta\sigma > 2\sigma_Y \end{cases} \tag{16}$$

Even though the above equation is self-consistent if $\Delta\sigma_n < 2\sigma_Y$, its mathematical formulation makes the numerical solution harder to obtain. In addition, it is not easy to obtain the yielding parameter σ_Y, because the calculation of the stress associated with "zero" residual strain will greatly depend on the resolution of the adopted measurement technique. In practice, since Ramberg-Osgood data is readily available for most materials, the above stress-strain relationship is not widely adopted in fatigue design.

The second procedure to avoid the errors induced by the classical Neuber approach is to use the Ramberg-Osgood model to describe not only the stresses at the notch root, but also to describe the ***nominal*** stresses, using

$$\frac{\Delta\varepsilon_n}{2} = \frac{\Delta\sigma_n}{2E} + \left(\frac{\Delta\sigma_n}{2H_c}\right)^{1/h_c} \tag{17}$$

Given $\Delta\sigma_n$, the stress range at the notch root $\Delta\sigma$ can be calculated from equations (1), (11), and (17), giving

$$K_t^2\left(\Delta\sigma_n^2 + \frac{2E\Delta\sigma_n^{(h_c+1)/h_c}}{(2H_c)^{1/h_c}}\right) = \Delta\sigma^2 + \frac{2E\Delta\sigma^{(h_c+1)/h_c}}{(2H_c)^{1/h_c}} \tag{18}$$

and then $\Delta\varepsilon$ is computed using

$$\Delta\varepsilon = \frac{\Delta\sigma}{E} + 2\left(\frac{\Delta\sigma}{2H_c}\right)^{1/h_c} \tag{19}$$

If equation (18) is applied to the SAE 1015 example discussed before, then the stress amplitude at the notch root can be calculated as $\Delta\sigma/2 \cong 573$MPa, a much more reasonable value for a nominal amplitude of 380MPa with $K_t = 3$.

Equation (17) should also be applied to the first 1/2 cycle of the loading, which has a different expression than the subsequent hysteresis loops, as shown in equation (9). This first 1/2 cycle departs from the origin of the σε plane following the cyclic σε curve. When elastic-plastic nominal stresses are considered, equation (9) becomes

$$K_t^2 \cdot \left(\sigma_{n_0}^2 + \frac{E\sigma_{n_0}^{(h_c+1)/h_c}}{H_c^{1/h_c}}\right) = \sigma_0^2 + \frac{E\sigma_0^{(h_c+1)/h_c}}{H_c^{1/h_c}} \quad (20)$$

Figure 2 shows a comparison between the predictions of the classical Neuber approach from equation (13) and the corrected ones from equation (18). The considered material is a hot-rolled SAE 1009 steel, with $h_c = 0.12$ and $H_c = 462$MPa [9], and the notch root has a K_t of 3. Note that the graph is only plotted until the stress amplitude calculated from equation (18) reaches the Coffin-Manson coefficient σ_c. Since a stress amplitude of σ_c is associated with a fatigue life of $N = 1/2$ cycle, it makes no physical sense to plot notch root stresses beyond this value. Also, for comparison purposes, all stresses are normalized using the material cyclic yielding strength S_{Yc}.

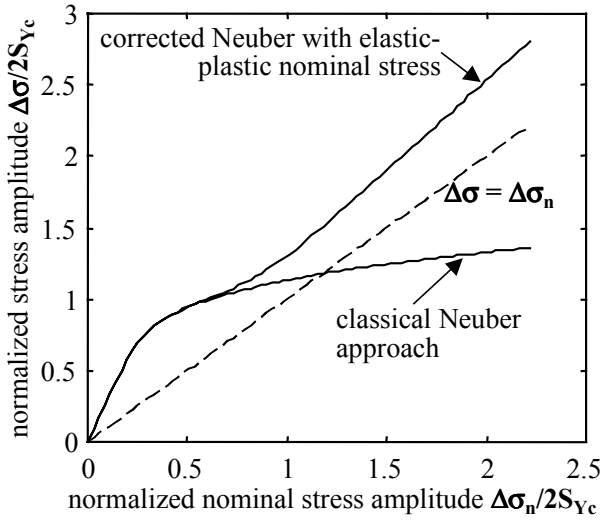

Figure 2. Stress amplitudes calculated by the classical and the corrected Neuber approaches (SAE 1009, $K_t = 3$).

As it can be seen in the figure, for nominal stress amplitudes $\Delta\sigma_n/2$ smaller than $0.5 \cdot S_{Yc}$ both predictions result in roughly the same notch root stress. For larger nominal stress values the predictions diverge, and after crossing the dashed line the classical Neuber approach wrongfully predicts notch root stresses ***smaller*** than the nominal stress.

Figure 3 plots the same graph for a different material, an SAE 1045 steel with 416 Brinell hardness, $h_c = 0.12$, and $H_c = 2235$MPa [9]. Since there is very little plastic deformation in this particular steel, both predictions resulted in roughly the same notch root stress. This lack of ductility can be seen in Figure 3, which shows that the considered specimen ($K_t = 3$) is expected to rupture for nominal stress amplitudes $\Delta\sigma_n/2$ slightly smaller than S_{Yc}.

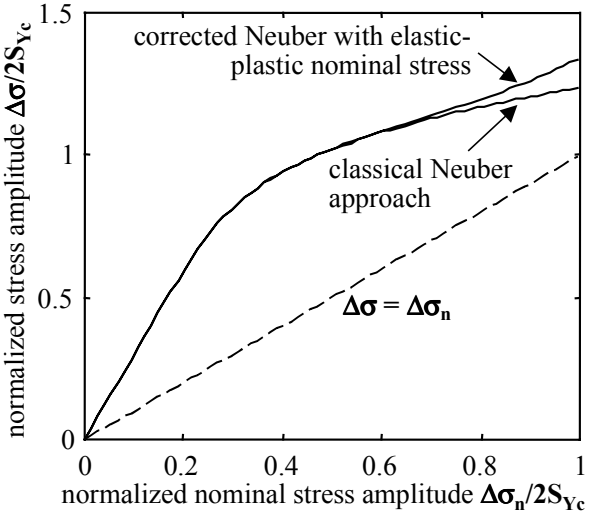

Figure 3. Stress amplitudes calculated by the classical and the corrected Neuber approaches (SAE 1045, $K_t = 3$).

However, if significant ductility is present in the considered material, then the classical Neuber approach will lead to increasing non-conservative errors as the nominal stress is increased. Figure 4 shows the stress concentration factor K_σ and the strain concentration factor K_ε calculated using both approaches for the hot-rolled SAE 1009 steel.

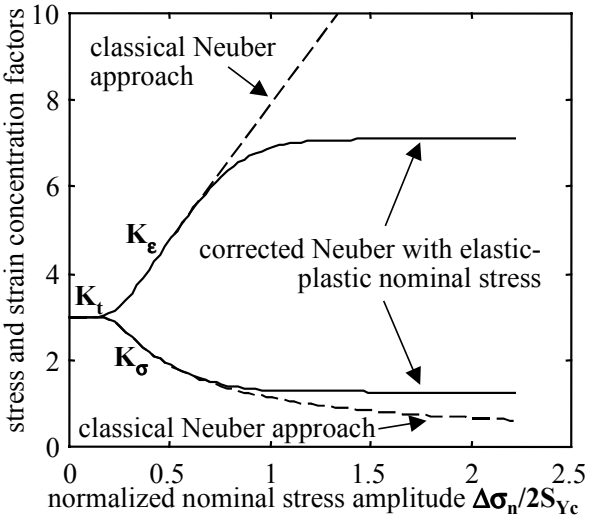

Figure 4. Stress and strain concentration factors calculated by both Neuber approaches (SAE 1009, $K_t = 3$).

From Figure 4, it can be seen that the classical Neuber approach predicts ever increasing strain concentration factors $\mathbf{K_\varepsilon}$, much higher than the correct ones calculated considering elastic-plastic nominal stresses. As expected, the wrong stress intensity factors $\mathbf{K_\sigma}$ calculated using elastic nominal stresses (lower dashed curve in the figure) can reach values smaller than 1, a non-sense as discussed before.

Note also that using the correct Neuber formulation, both $\mathbf{K_\sigma}$ and $\mathbf{K_\varepsilon}$ tend to a constant value as the nominal stress amplitude is increased. According to Neuber's rule, any material that follows Ramberg-Osgood's equation presents this same behavior. These constant values can be calculated from equation (18), assuming that the elastic component of both nominal and notch-root strains are negligible compared to the respective plastic strain components, resulting in

$$K_t^2\left(\frac{2E\Delta\sigma_n^{(h_c+1)/h_c}}{(2H_c)^{1/h_c}}\right)=\frac{2E\Delta\sigma^{(h_c+1)/h_c}}{(2H_c)^{1/h_c}}$$

$$\Rightarrow K_\sigma=\frac{\Delta\sigma}{\Delta\sigma_n}=K_t^{\,2h_c/(1+h_c)} \qquad (21)$$

From equation (21) and using that $\mathbf{K_\sigma \cdot K_\varepsilon} = \mathbf{K_t}^2$, then lower and upper bounds can be calculated for $\mathbf{K_\sigma}$ and $\mathbf{K_\varepsilon}$

$$K_t^{\,2h_c/(1+h_c)} \le K_\sigma \le K_t \qquad (22)$$

$$K_t \le K_\varepsilon \le K_t^{\,2/(1+h_c)} \qquad (23)$$

Since the cyclic hardening exponent $\mathbf{h_c}$ varies very little (between 0.05 and 0.3), equation (22) results in an interesting lower bound for the stress concentration factor in structural steels, namely

$$K_\sigma \ge K_t^{0.1} \text{ to } K_t^{0.46} \qquad (24)$$

For instance, according to equation (24), a circular hole ($\mathbf{K_t} = 3$) in most structural steels results in stress concentration factors $\mathbf{K_\sigma}$ with a lower bound between 1.12 to 1.66. In this case, if the considered material has $\mathbf{h_c}$ between 0.05 and 0.3, then $\mathbf{K_\sigma}$ values smaller that 1.12 are very likely a result of inaccurate Neuber formulations such as the one in equation (13).

To ***quantitatively*** account for the errors induced by the Hookean modeling of the nominal stresses, the error in the stress range $\Delta\sigma$ calculated using equation (13) is investigated next. Figure 5 shows the dependency of the error in $\Delta\sigma$ with the geometric stress concentration factor $\mathbf{K_t}$ for the hot-rolled SAE 1009 steel described before.

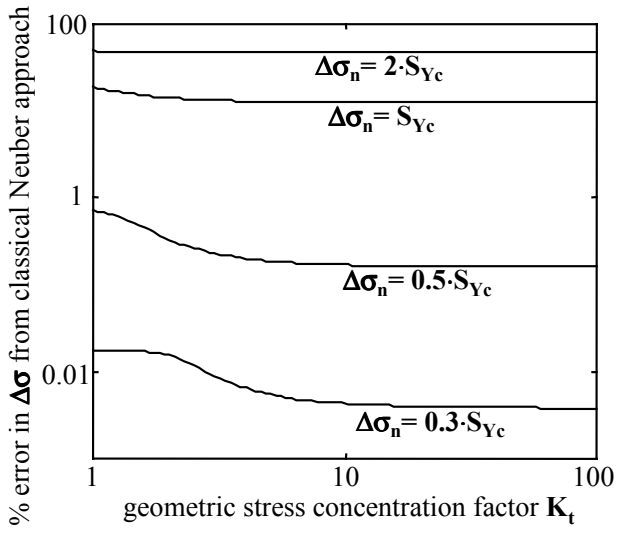

Figure 5. Errors in the stress range calculated using the classical Neuber approach (SAE 1009, $\mathbf{K_t}$ = 1 to 100).

As it can be seen above, the errors in $\Delta\sigma$ are not a strong function of $\mathbf{K_t}$, being mainly dependent on the nominal stress range $\Delta\sigma_n$. These errors tend to slightly decrease as $\mathbf{K_t}$ is increased, reaching a constant value for very high stress concentration factors.

To better quantify these errors, a detailed study has been performed on measured properties of 517 different structural steels. Figures 6 and 7 show the percentage error in the stress ranges calculated by the classical Neuber approach for these 517 steels, considering $\mathbf{K_t}$ = 3. All curves are only plotted until the corrected stress amplitude at the notch root reaches the Coffin-Manson parameter σ_c (when the specimen is assumed to rupture).

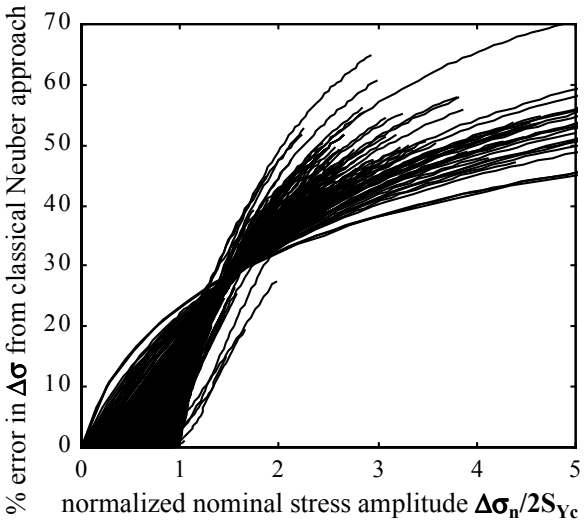

Figure 6. Errors in the stress range calculated using the classical Neuber approach (**517 steels**, $\mathbf{K_t}$ = 3).

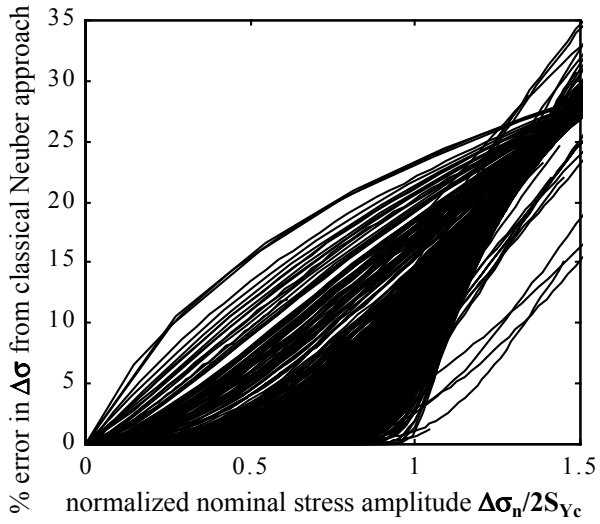

Figure 7. Errors in the stress range, zoomed at nominal stress amplitudes below $\mathbf{S_{Yc}}$ (**517 steels**, $\mathbf{K_t}$ = 3).

Figure 6 shows that the Hookean modeling can lead to errors higher than 70% in the calculated stress at the notch root, especially if the nominal stress amplitude $\Delta\sigma_n/2$ is much above the cyclic yielding strength $\mathbf{S_{Yc}}$. However, even if the nominal stresses are much smaller than $\mathbf{S_{Yc}}$, the errors induced by the classical Neuber approach are very significant, reaching values up to 23% in some cases (see Figure 7). And due to the non-linearities of the Coffin-Manson rule, these errors in stress translate to much higher non-conservative errors in life prediction. To visualize this, Figures 8 and 9 show the errors in the life predicted by the classical Neuber approach, calculated from measured Coffin-Manson data of the 517 structural steels.

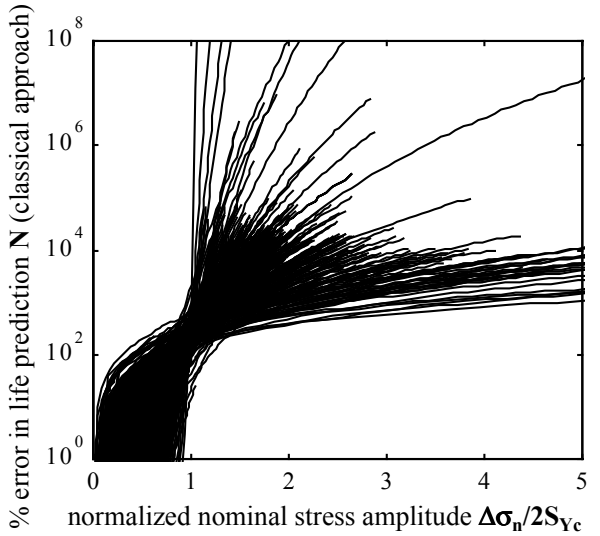

Figure 8. **Non-conservative** errors in the life predicted by the classical Neuber approach (**517 steels**, $\mathbf{K_t}$ = 3).

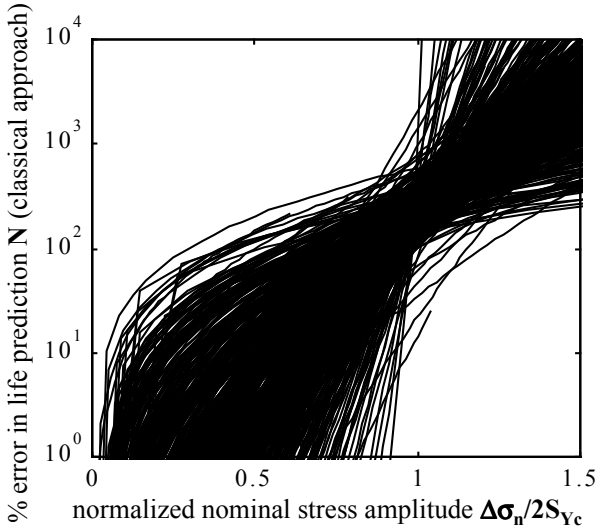

Figure 9. Errors in the predicted life, zoomed at nominal stress amplitudes below $\mathbf{S_{Yc}}$ (**517 steels**, $\mathbf{K_t}$ = 3).

As it can be seen in Figure 8, inadmissible ***non-conservative*** life prediction errors can be generated by using equation (13). In addition, significant non-conservative errors may be present for virtually any nominal stress amplitude, even for those well under $\mathbf{S_{Yc}}$. For instance, nominal stress amplitudes of only $0.3\cdot\mathbf{S_{Yc}}$ can lead to errors higher than 100% in life prediction, while values close to $\mathbf{S_{Yc}}$ may result in errors up to 2,000%. Depending on the considered material, even nominal stresses as low as $0.1\cdot\mathbf{S_{Yc}}$ can result in significant non-conservative errors. Table 1 summarizes the maximum prediction errors obtained at several nominal stress levels.

Table 1. ***Non-conservative*** errors in the predicted stress and life from the classical Neuber approach (**517 steels**).

$\frac{\Delta\sigma_n}{2}$	maximum errors in $\Delta\sigma$	maximum errors in **N**
$0.1\cdot\mathbf{S_{Yc}}$	5%	27%
$0.3\cdot\mathbf{S_{Yc}}$	11%	102%
$0.5\cdot\mathbf{S_{Yc}}$	15%	202%
$0.8\cdot\mathbf{S_{Yc}}$	21%	411%
$\mathbf{S_{Yc}}$	23%	2081%
at rupture	74%	10^{12} %

In summary, the alarming prediction shown in Table 1 implies that it is mandatory to use Ramberg-Osgood to model **both** the nominal and the critical stresses and strains, as shown in equation (18), otherwise completely wrong life predictions may be obtained.

In addition to its application to the εN method, the corrected Neuber approach can be very useful to improve

the accuracy of the SN method. This procedure is highly recommended when residual stresses are present in the specimen, caused by unexpected overloads (or underloads) that induce plastic deformation. If only a few of those plastic events occur in the loading history, it is not necessary to switch from the SN method to a much more complex εN methodology. Instead, the SN method can still be applied to the events that do not cause macroscopic plastic deformation, while the overloads are accounted for by using the corrected Neuber rule in concert with Coffin-Manson. The residual stresses calculated by the Neuber rule must then be added to the mean component of the subsequent load events, so that the SN method can account for interaction effects among cycles. The next section describes how the residual stress effect can be included in the SN method.

RESIDUAL STRESS EFFECT IN THE SN METHOD

To increase the SN prediction accuracy and to remove one of the main Miner's rule shortcomings, it is possible to modify the traditional SN methodology to consider plasticity induced loading sequence effects. The idea is simple (but not easy to be computationally implemented), and can be summarized as follows.

First, the initial residual stress state must be known at the critical point. Residual stresses act as mean loads, and must be added to each mean stress component $\sigma_{m,i}$. The complex load must then be counted by the sequential rain-flow method, a variation of the traditional rain-flow algorithm that preserves load sequence information [15]. Every load peak $\sigma_{max,i}$ (calculated from the sum of $\sigma_{m,i}$, of the alternate stress component $\sigma_{a,i}$, and of the residual stress σ_{res}) must be compared to the cyclic yielding strength S_{Yc}. If $\sigma_{max,i} > S_{Yc}$ there is yielding at the notch root, and the procedure should at that instant change from the SN to the sequential εN method, to calculate not only the damage but also the change in the residual stress state induced by that load event. The sequential εN method keeps track of the correct hysteresis loops at the notch root. Then the procedure can turn back to the SN method, bringing the new σ_{res} value to continue the damage calculations as before. The main advantage of this hybrid method is its computational efficiency, as the SN equations are much simpler to solve than the εN equations.

For instance, consider a specimen with $K_t = 3$, made of an SAE 1015 steel, with hardening properties $h_c = 0.22$ and $H_c = 945$MPa [9]. Let's calculate the residual stress at the notch root caused by a nominal loading history of $\sigma_n = \{0 \rightarrow 100 \rightarrow 0\}$ **MPa**. To calculate the critical stress after the first 1/2 cycle, equation (20) is solved considering $\sigma_{n0} = 100$MPa, resulting in $\sigma_0 \cong 214$MPa. The unloading part is then calculated using the correct Neuber formulation from equation (18), considering $\Delta\sigma_n = 100$MPa, resulting in $\Delta\sigma \cong 272$MPa. Therefore, the calculated residual stress at the notch root is $\sigma_{res} = \sigma_0 - \Delta\sigma = -58$MPa. This compressive σ_{res} must then be added to the mean component of the subsequent loadings, which will lead to an increased fatigue life and a much more accurate SN prediction.

Note that the maximum stress at the notch root in this example is 214MPa, which is ***smaller*** than both monotonic and cyclic yielding strengths for the considered SAE 1015 steel ($S_Y = 228$MPa, $S_{Yc} = 241$MPa). Classical SN methodology would ignore such residual stress, especially because the maximum stress at the critical point is below S_Y. However, a residual stress of about 25% of the yielding strength is very significant to the fatigue life of the specimen and cannot be neglected. In addition, if the calculated σ_{res} was positive (tensile), then non-conservative errors could result from neglecting such effects.

Finally, it is important to emphasize that the corrected Neuber approach from equations (18) and (20) should be used in the above calculations, since it was shown that the Hookean modeling of the nominal stresses can result in wrong predictions. Therefore, the proposed corrections to **both** the Neuber approach and the SN methodology must be applied even for nominal and critical stresses significantly smaller than S_Y, under the penalty of making highly ***non-conservative*** fatigue life predictions.

However, the numerical solution of the correct Neuber rule (considering elastic-plastic nominal stresses) is not trivial to implement, especially when complex loads are involved. The next section presents the methodology required to warrant correct numerical predictions of the critical loops considering elastic-plastic nominal stresses.

NUMERICAL IMPLEMENTATION OF THE εN METHOD

NUMERICAL SOLUTION OF COFFIN MANSON AND NEUBER EQUATIONS – To solve equations (3), (18), and (20), a numerical method has been developed based on the fact that those equations essentially constitute the combination of two straight lines when represented in bi-logarithmic scale. Since the Newton-Raphson method is very efficient to solve equations with approximately constant derivative, it was adapted to the bi-logarithmic scale. First, the Neuber and Coffin-Manson equations are represented in a general parametric form

$$\delta = \beta \cdot e^{B.x} + \gamma e^{C.x} \qquad (25)$$

where **x** is the unknown to be calculated numerically, **e** is equal to 2.71828, and δ, β, **B**, γ, and **C** are equation parameters. In the case of the Coffin-Manson equation (3), the unknown **x** and the equation parameters are defined as

$$\delta = \frac{\Delta\varepsilon}{2},\ \beta = \frac{\sigma_c}{E},\ B = b,\qquad \gamma = \varepsilon_c,\ C = c,\ x = \ln(2N) \tag{26}$$

For Neuber's rule, its simplified version shown in equation (13) can be represented using the parameters

$$\delta = (K_t\,\Delta\sigma_n)^2,\ \beta = 1,\ B = 2,\qquad \gamma = \frac{2E}{(2H_c)^{1/h_c}},\ C = 1 + \frac{1}{h_c},\ x = \ln(\Delta\sigma_i) \tag{27}$$

while the corrected equation (18) is defined using

$$\delta = K_t^2\left(\Delta\sigma_n^2 + \frac{2E\Delta\sigma_n^{(h_c+1)/h_c}}{(2H_c)^{1/h_c}}\right),\ \beta = 1,\ B = 2,\qquad \gamma = \frac{2E}{(2H_c)^{1/h_c}},\ C = 1 + \frac{1}{h_c},\ x = \ln(\Delta\sigma_i) \tag{28}$$

and equation (20) for the first 1/2 cycle is represented by

$$\delta = K_t^2\left(\sigma_{n_0}^2 + \frac{E\cdot\sigma_{n_0}^{(h_c+1)/h_c}}{H_c^{1/h_c}}\right),\ \beta = 1,\ B = 2,\qquad \gamma = \frac{E}{H_c^{1/h_c}},\ C = 1 + \frac{1}{h_c},\ x = \ln(\sigma_0) \tag{29}$$

The procedure for the solution of equation (25) can be summarized by:

- finding the value for x_0 for the first iteration through

$$x_0 = \min\left(\frac{\ln(\delta/\beta)}{B}, \frac{\ln(\delta/\gamma)}{C}\right) \tag{30}$$

where the **min** function returns the smaller between two values, and **ln** is the natural logarithm function. In the case of the Coffin-Manson rule, equation (30) evaluates if the strain range is in the predominantly elastic or plastic region, taking as initial value the closest one to the solution.

- calculating the value of x_{i+1} of the next iteration as a function of the x_i value ($i \geq 0$)

$$x_{i+1} = x_i - \left(\frac{\beta e^{Bx_i} + \gamma e^{Cx_i}}{\beta B e^{Bx_i} + \gamma C e^{Cx_i}}\right)\cdot\ln\left[\frac{\beta e^{Bx_i} + \gamma e^{Cx_i}}{\delta}\right] \tag{31}$$

- defining $(\xi - 1)$ as the maximum allowable relative error, the iterations proceed until the expression

$$\ln\left[\frac{\left(\beta e^{B(x_i + \ln(\xi))} + \gamma e^{C(x_i + \ln(\xi))}\right)}{\delta}\right] \tag{32}$$

is negative. To exemplify the usage of this method, the remaining life of a steel specimen is calculated considering properties E = 203GPa, σ_c = 896MPa, ε_c = 0.41, b = –0.12, and c = –0.51. From equation (3), for a strain range $\Delta\varepsilon$ = 2000με and a maximum error of 0.1% (ξ = 1.001),

$$x_0 = 6.60;\ x_1 = 11.12;\ x_2 = 11.87;\ x_3 = 11.91$$
$$\Rightarrow\ 2N = e^{11.91} = 149{,}000 \text{ reversions}$$

Thus the process converges within only 3 iterations. If the traditional Newton-Raphson method had been used, considering an initial value of 1 for 2N, 15 iterations would be necessary to calculate the solution within the 0.1% accuracy. Moreover, even if the initial condition defined in equation (30) had been used, the Newton-Raphson method would still need 10 iterations to converge.

In summary, the numerical procedure shown in this section is able to solve fast and accurately both the Coffin-Manson equation and the Neuber rule considering elastic-plastic nominal stresses. The enabling methodology presented in this work has been successfully implemented on a general-purpose fatigue design program named **ViDa**, described next.

THE **ViDa** SOFTWARE – To automate the fatigue design routines by all local methods, a powerful software named **ViDa** has been developed [16]. It runs on Windows environments, has an intuitive and friendly graphical interface, is particularly useful to deal with complex loads considering sequence effects both in the initiation and in the propagation of one and two-dimensional (1D and 2D) fatigue cracks, and, among several others, includes all features discussed in this paper. Of particular academic interest are the innovations that had to be developed and implemented in the several fatigue design methods and computation routines to guarantee the reliability and to increase the speed of the calculations, such as:

- introduction of the ordered rain-flow counting method;
- the consideration of elastic-plastic overload effects on the SN method;
- a series of corrections in the traditional εN methodology, to guarantee the prediction of physically acceptable elastic-plastic hysteresis loops at a notch root;
- 1D and 2D crack propagation models with adjustable speed and precision;
- numerical filters to improve calculation efficiency;
- models to predict fatigue crack propagation and arrest after overloads;
- several extensive and resourceful databases;
- intuitive graphical interface and traditional notation, to eliminate any programming from the design process.

To guarantee the precision of the εN method calculations, the **ViDa** software includes **all** the corrections discussed in this work, besides a series of other equally important features such as:

- it draws the εN curve and plots over it the traditional SN curve for comparison purposes, and it can force the elastic component of the εN curve to reach the fatigue limit at any specified life;
- it allows the Neuber rule to be changed by the linear strain concentration rule;
- it calculates and draws the properly corrected hysteresis loops, but it can also calculate them by the non-sequential εN method;
- it calculates fatigue life by five methods: Coffin-Manson, Manson's universal slopes, Morrow elastic, Morrow elastic-plastic and Smith-Topper-Watson, considering all the loop corrections;
- it generates graphs of damage versus event for each one of the calculation models.

To illustrate the accuracy of these predictions, Figure 10 compares predicted and experimental loops measured in API S-135 steel under complex load.

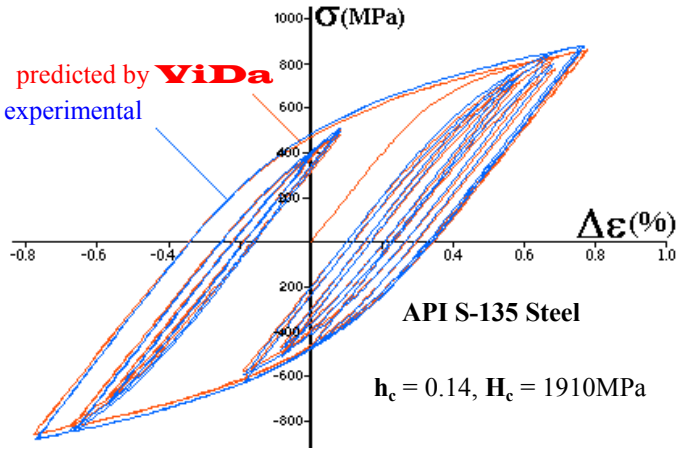

Figure 10. Predicted and experimentally measured stabilized loops generated under complex loading [17].

CONCLUSIONS

This paper studied some inconsistencies in the traditional εN procedures, in particular when modeling nominal stresses by Hooke's law and the stresses and strains at the critical notch root by Ramberg-Osgood's equation. From a study on measured properties of 517 structural steels, it was found that ***non-conservative*** life prediction errors as high as 2000% can be obtained if the nominal stresses are modeled as purely elastic, even if such stresses are significantly ***below*** the material yielding strength. The correct formulation for the Neuber rule was presented, considering elastic-plastic nominal stresses, and an effective procedure for its numerical solution has been introduced. All the presented methodologies have been verified and implemented on a general-purpose fatigue design program, developed to predict both initiation and propagation fatigue lives under complex loading by all classical design methods.

REFERENCES

[1] Bannantine, J.A., Comer, J.J., Handrock, J.L., *Fundamentals of Metal Fatigue Analysis*, Prentice Hall 1990.

[2] Duggan, T.V., Byrne, J., *Fatigue as a Design Criterion*, Macmillan 1977.

[3] Dowling, N.E., *Mechanical Behavior of Materials*, Prentice-Hall 1993.

[4] Farahmand, B., *Fatigue and Fracture Mechanics of High Risk Parts*, Chapman & Hall 1997.

[5] Fuchs, H.O., Stephens, R.I., *Metal Fatigue in Engineering*, Wiley 1980.

[6] Hertzberg, R.W., *Deformation and Fracture Mechanics of Engineering Materials*, Wiley 1989.

[7] Manson, S.S. "Fatigue: A Complex Subject - Some Simple Approximations", *Experimental Mechanics*, v.5 n.4, pp.193-226, 1965.

[8] Mitchell, M.R., "Fundamentals of Modern Fatigue Analysis for Design", in *Fatigue and Microstructure*, ASM 1979.

[9] Rice, R.C., ed., *Fatigue Design Handbook*, SAE 1988.

[10] Sandor, B.I., *Fundamentals of Cyclic Stress and Strain*, University of Wisconsin 1972.

[11] Castro, J.T.P., Meggiolaro, M.A., "Some Comments on the εN Method Automation for Fatigue Dimensioning under Complex Loading," (in Portuguese), *Revista Brasileira de Ciências Mecânicas*, v. 21, pp.294-312, 1999.

[12] Castro, J.T.P., Meggiolaro, M.A., *Projeto à Fadiga sob Cargas Complexas* (in Portuguese), PUC-Rio 2001.

[13] Castro, J.T.P., Meggiolaro, M.A., "Automation of the Fatigue Design Under Complex Loading," I Int. Fatigue Seminar SAE-Brasil, 2000-01-3334, 2000.

[14] Topper, T.H., Wetzel, R.M., Morrow, JoDean, "Neuber's Rule Applied to Fatigue of Notched Specimens," *Journal of Materials*, v. 4, no. 1, pp.200-209, 1969.

[15] Miranda, A.C.O., Meggiolaro, M.A., Castro, J.T.P., Martha, L.F., Bittencourt, T.N., "Fatigue Crack Propagation under Complex Loading in Arbitrary 2D Geometries," *Appl. of Autom. Tech. in Fatigue and Fract. Testing and Analysis*, ASTM STP 1411, 2001.

[16] Meggiolaro, M.A., Castro, J.T.P., "ViDa 98 – a Visual Damagemeter to Automatize the Fatigue Design under Complex Loading," (in Portuguese), *Revista Brasileira de Ciências Mecânicas*, v. 20, pp.666-685, 1998.

[17] Guizzo, T. "Laços de Histerese Elastoplásticos Gerados sob Carregamentos Complexos," M.Sc. Thesis, Mech. Eng. Dept. PUC-Rio, 1999.